Journal of Applied Polymer Science

Meticulous Analysis and Consequences of Microstructure Changes on Melt Rheology and Dynamic Viscoelasticity of Thermoplastic Vulcanizates upon Reprocessing

Pranab Dey,[1] Kinsuk Naskar,[1] Golok B. Nando,[1] Biswaranjan Dash,[2] Sujith Nair,[2] G. Unnikrishnan[2]
[1]Rubber Technology Centre, Indian Institute of Technology Kharagpur, Kharagpur, India
[2]CEAT Limited, Chandrapura, Halol, Panchmahal, Gujarat, India
Correspondence to: K. Naskar (E-mail: knaskar@rtc.iitkgp.ernet.in)

ABSTRACT: Thermoplastic vulcanizates (TPVs), which are a special class of elastomer alloy, prepared by dynamic vulcanization possess unique morphology of finely dispersed micron-size cross-linked elastomeric particles in a continuous thermoplastic matrix. The present study investigates the microstructure formation of elastomeric phase and its associated morphological changes during reprocessing of TPVs based on poly[styrene-*b*-(ethylene-*co*-butylene)-*b*-styrene] triblock co-polymer (S-EB-S) and solution polymerized styrene butadiene elastomer (S-SBR) by scanning electron microscopy and atomic force microscopy. Semi-efficient and efficient sulfur-based curing systems have been adopted to cure the elastomeric phase and a comparative study has been made to demonstrate and explain the effect of reprocessing on the melt rheology and dynamic viscoelasticity of the TPVs. The present work also provides a better insight and guidance to control the microstructure of the cross-linked elastomeric phase to prepare selectively co-continuous or dispersed phase morphology. © 2014 Wiley Periodicals, Inc. J. Appl. Polym. Sci. **2014**, *131*, 41182.

KEYWORDS: blends; elastomers; morphology; rheology; rubber

Received 10 April 2014; accepted 18 June 2014
DOI: 10.1002/app.41182

INTRODUCTION

Thermoplastic vulcanizates (TPVs) are a specific group of elastomer alloy[1] where the elastomeric phase is selectively cross-linked by dynamic vulcanization and dispersed in the presence of a molten thermoplastic phase under intensive mixing.[2] It exhibits elastomer-like properties: such as lower compression set, lower stiffness, greater resistance to fatigue, better resistance to heat and chemicals and so forth[3,4] as well as the melt-processability like thermoplastics. These phenomenal qualities led themselves as a potential competitor to the fast growing rubber market[5] for the last two decades and gaining considerable attraction from various industries such as automotives, electronics, buildings and so forth.

S-EB-S is a hydrogenated styrenic triblock co-polymer which is primarily used as a compatibilizer for the binary blend systems.[6] However, several researchers have reported the blend of S-EB-S with polypropylene (PP) to prepare TPEs.[7,8] Sengupta et al. reported the comparative study of the oil extended S-EB-S/PP blend with PP/EPDM TPV.[9,10] Sengers et al. investigated the rheological properties of PP/S-EB-S blends.[11,12] Later on Ahmad et al. prepared highly transparent TPE from isotactic PP and S-EB-S triblock co-polymer.[13] Picchioni et al. studied the mechanical and thermal behavior of polystyrene (PS)/S-EB-S blend.[14] Therefore, to the best of our knowledge, there is no literature available which in-detail investigated the microstructure changes of the sulfur cured elastomeric phase upon reprocessing. The solubility parameters of both S-EB-S and S-SBR are rather comparable and thus it was presumed that the dynamic vulcanization would result in such a TPV which can meet the growing demands for industrial applications.

The sulfur vulcanization of the elastomeric phase in the TPVs can be achieved in three different ways viz. efficient vulcanization system (EV), semi-efficient vulcanization system (SEV), and conventional vulcanization system (CV). EV systems are those where a low level of sulfur and a correspondingly high level of accelerator or sulfurless curing are employed in vulcanizates for which an extremely high heat and reversion resistance is required. In the CV systems, the sulfur dosage is high and correspondingly the accelerator level is low. The CV systems provide better flex and dynamic properties but worse thermal and reversion resistance. For optimum levels of mechanical and dynamic properties of vulcanizates with intermediate heat, reversion, flex and dynamic properties, the so-called SEV systems with an intermediate level of accelerator and sulfur are employed.

Table I. Compounding Recipe of S-EB-S/ S-SBR TPVs (In phr)

Ingredients	Function	Sample ID	
		SST 1	SST 2
S-SBR	Elastomer	100	100
S-EB-S	Thermoplastic elastomer	100	100
ZnO	Accelerator activator	4	4
Stearic acid	Accelerator activator	1	1
CBS	Accelerator	1	1
TMTD	Accelerator	-	0.5
Sulfur	Cross-linking agent	1	1

phr, parts per hundred parts of elastomer.

The primary objective of this investigation is to correlate the melt rheology, dynamic viscoelasticity, and physico-mechanical properties with cross-link density as well as micro-structural changes of the cross-linked elastomeric phase upon reprocessing of the respective TPVs.

EXPERIMENTAL

Materials

S-EB-S (trade name Kraton® G1657) is a clear, linear triblock co-polymer based on styrene and ethylene/butylene with a polystyrene content of 13%. Density of S-EB-S is 0.90 gm/cc and the melt flow index is 22 gms/10 min at 230°C/5 kg. It is supplied by Kraton Polymer from Belgium in the physical form of dusted pellet. Another polymer, that is, S-SBR has been procured from Dycon Chemicals, Mumbai, India having a polystyrene content of 23.5%. The solvent toluene was obtained from Merck Specialities Private, India. Accelerator activators, that is, zinc oxide (zinc content 82%) and stearic acid (maximum ash content 0.1%) were procured from Sunrise Overseas, India. Accelerators N-cyclohexyl-2-benzothiazolesulfenamide and tetramethyl thiuram disulfide having melting point 98 and 142°C as well as ash content below 3%, respectively were obtained from Lanxess Rubber Chemicals, India. Finally, the cross-linking agent sulfur powder (maximum ash content 0.2%) was procured from Triveni Chemicals, India.

Preparation of TPVs

Binary blended TPVs with a composition of 50/50 wt % S-EB-S/S-SBR were prepared using a Brabender Plastograph EC (Digital 3.8 KW motor, a torque measuring range of 200 Nm and a speed range from 0.2 to 150/min). Mixing was carried out at 160°C at a rotor speed of 60 rpm. To make the TPVs (Table I), S-EB-S was first loaded into the chamber and allowed to melt in the mixer for 2 min, and then S-SBR was added and melt-blended according to the specified conditions which took about 1 min. Thereafter, zinc oxide and stearic acid were added and finally the sequence ended up with the addition of sulfur and accelerator. Mixing was continued until the plateau mixing torque was reached and the resulting TPVs were then quickly removed and passed through a two-roll mill having a close nip-gap at room temperature and then sheeted out for subsequent operations. The torque–time curves obtained during the melt blending process of TPV formation are given in Figure 1. The delta-torque value obtained has appeared to be higher for EV cured system and numerically the delta-torque difference is about 4.2 Nm for the mentioned TPVs.

Preparation of Moulded Specimens

The sheet obtained from the two-roll mill was compression moulded in a hydraulic press (Moore Presses, George E. Moore & Sons Birmingham, UK) at 160°C for 4 min, under a pressure of 5 MPa, to form tensile sheets of about 2 mm thick. The mould was allowed to cool under pressure to the ambient temperature before ejecting the sheets from the mould cavity. Dumb-bell specimens were punched out of the sheets using standard cutting die.

Reprocessing of Dynamically Cured TPVs

The principal advantage of TPVs over conventional systems is the possibility of reprocessing. To evaluate the reprocessability, all the moulded specimens (used while testing) were milled and then cut into small pieces. The material was then pelleticized by an extrusion process (Brabender lab-compounder 20/40 EC, Digital 5.2 KW motor, a torque measuring range of 2×40 Nm and a speed range from 1 to 600/min) with a die temperature of 160°C and a Brabender pelletizer unit (inverter drive motor and a standard speed of 0.5–15 m/min). Remaining all other zones excluding the feeding zone was set at 150°C; whereas, the initial set temperature for the feeding zone was set at 130°C. The resulting pellets thus obtained were reprocessed[15–17] in the Brabender internal mixer and subsequently their properties were measured with the moulded specimens to ensure the reprocessability.

Mechanical Properties

The mechanical properties of the blends were determined as per ASTM D 412 (A dumbbell specimen was placed in the grips of the testing machine, using care to adjust the specimen symmetrically to distribute tension uniformly over the cross section) using a Hounsfield H25KS universal testing machine at a cross-head speed of 500 mm/min. The hardness of the samples was determined using a Shore A Durometer hardness tester as per

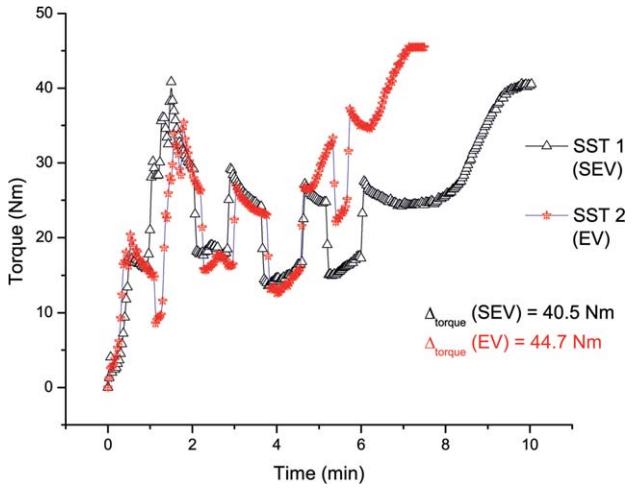

Figure 1. Torque–time curves for S-SBR/S-EB-S TPVs. [Color figure can be viewed in the online issue, which is available at wileyonlinelibrary.com.]

ASTM D 2240 (specimens having min 6 mm of thickness were subjected to the direct indentation through parallel contact of the specimen to the durometer pressure foot without shock and with just sufficient force to overcome the spring force). Testing of all the samples was carried out at 25°C.

Characterization

Overall Crosslink Density by Equilibrium Solvent Swelling Method. Swelling experiments were conducted on small rectangular (approximately 20 × 10 × 2 mm) specimens in toluene at room temperature for 1 week. At the end of immersion period the sample was removed, gently wiped with tissue and transferred to the weighing balance to obtain the swollen weight of the sample. From the degree of swelling an overall cross-link density (CLD) was calculated by using Flory–Rehner equation[18–20] (eq. (1)) relative to the (S-SBR+S-EB-S) phases as expressed by (v + S-EB-S). The latter was done in order to correct for a part of the S-EB-S, being extracted as amorphous phase.[21,22]

$$(v+\text{S-EB-S}) = -\frac{1}{V_s} \times \frac{\ln(1-V_r)+V_r+\chi(V_r)^2}{(V_r)^{1/3}-0.5\times V_r}, \quad (1)$$

where,

(v + S-EB-S) = number of moles of effectively elastic chains per unit volume of S-SBR [mol/mL] (CLD) in presence of S-EB-S.

V_s = molar volume of solvent (toluene).

χ = polymer-swelling agent interaction parameter, taken as 0.38 for both S-SBR and toluene at 25°C.[23,24]

V_r =Volume fraction of rubber in the swollen network and V_r can be expressed as

$$V_r = \frac{1}{A_r+1}, \quad (2)$$

where,

A_r = Ratio of the volume of absorbed toluene to that of S-SBR after swelling.

Scanning Electron Microscopy. ZEISS EVO 60 (Carl ZEISS SMT, Germany) scanning electron microscopy (SEM) was used to study the surface topography of the cryogenically fractured specimens after complete etching of the TPE phase (S-EB-S) using toluene solvent at 25°C for 72 hrs. The etched specimens were then subjected to SEM micrography after evaporating the solvent at 60°C for 24 hrs.

Atomic Force Microscopy. Intermittent contact mode atomic force microscopy, ACAFM (Agilent 5500 Scanning Probe Microscope) was used to investigate the morphology of the TPVs thin films prepared by compression moulding at 5 MPa pressure at 160°C for 4 min in support to the SEM observations. The resonance frequency of the tip was 146–236 kHz and the force constant was 48 N/m.

Melt Rheological Study. The rheological measurements of TPVs were carried out by a Rubber Process Analyzer (RPA 2000; Alpha Technology). Frequency range was selected between 0.5 and 32 Hz and a strain controlled dynamic frequency sweep test was applied. Similarly, for frequency controlled dynamic strain sweep, the strain range was selected in between 0.7 and 1250%. The measurements were done in ambient atmosphere at a temperature of 120°C. During each experiment, the temperature was maintained at the desired constant value by heating of the sample.

Dynamic Mechanical Analysis. ***Creep study.*** Creep compliance measurements were performed with a Dynamic Mechanical Analyzer, Metravib 50 N, France. The creep experiments were carried out using tension mode of the DMA instrument. The samples were subjected to a constant stress of 0.3 MPa, and the resulting strain and its recovery were recorded at 25°C. Compliance D(t) was calculated from the stress and strain data[25] using eq. 3.

$$D(t) = \frac{\varepsilon(t)}{\sigma_0}, \quad (3)$$

where ε(t) and σ_0 are respectively strain and stress on the sample.

Stress relaxation study. Stress relaxation experiments were carried out using tension mode of the DMA instrument at the temperature of 25°C. The samples were subjected to a constant strain of 0.05%, and the resulting stress and its recovery were recorded. Relaxation modulus E(t) was calculated from the stress and strain data[25] using eq. 4.

$$E(t) = \frac{\sigma_t(t)}{\varepsilon_0}, \quad (4)$$

where $\sigma_t(t)$ and ε_0 are respectively stress and strain on the sample.

RESULTS AND DISCUSSION

Mixing Torque and Reprocessability of TPVs Containing Sulfur Cured Elastomeric Phase

Mixing torque gives an idea of shear and elongational flow in actual mixing environment. Figure 1 depicts the change in mixing torque with time during dynamic vulcanization for the SEV (SST 1) and EV (SST 2) cured TPVs. Delta torque ($\Delta_{torq.}$) value obtained for EV and SEV cured TPVs are 44.7 and 40.5 Nm, respectively. An increase in torque is observed with the addition of sulfur, indicating the cross-linking of S-SBR elastomer phase. Higher accelerator content (SST 2) results in a stronger increase in mixing torque, which suggests the formation of higher CLD. The same observation has been proven experimentally and shown later. As shown in Figure 1, the mixing torque levels off at the end of dynamic vulcanization which indicates that the system is still melt processable even after the formation of cross-linked elastomeric phase.[26] At this stage, the cross-linked elastomeric droplets are getting dispersed in the TPE matrix and due to attainment of higher elasticity the shear rate acting on it is not higher enough to facilitate further break down of the elastic network. Therefore, it eventually ends up with a constant torque level due to the slippage of cross-linked elastomeric particles at the rotor surface and the chamber wall while floating into the TPE matrix. The dynamically vulcanized samples were successfully melt-pressed to a thin sheet and correspondingly mechanical (Table II) and dynamic properties have been measured. Moreover, the system was reprocessed with ease; the

Table II. Mechanical Properties of Sulfur Cured TPVs

Sample name	Tensile strength (MPa)	EB (%)	100% Modulus (MPa)	200% Modulus (MPa)	300% Modulus (MPa)	Hardness (shore A)
SST 1	4.9 (0.62)	672 (79.79)	0.9 (0.03)	1.4 (0.03)	2.0 (0.05)	52 (0.84)
SST 2	4.8 (0.38)	533 (42.03)	1.1 (0.03)	1.7 (0.06)	2.6 (0.09)	55 (0.71)

Standard deviation values for five numbers of test specimens are given in parenthesis.

moulded sheet has been torn off and pelleticized which was followed by reprocessing through internal mixer and then compression moulded to thin sheet. After reprocessing the mechanical properties have been measured and are given in Table III(a, b) for SEV and EV cured TPVs, respectively.

Overall Cross-Link Density by Equilibrium Solvent Swelling Method

Table III(a) indicates an improvement in mechanical properties while reprocessing for SEV cured TPVs unlike the case for EV cured TPVs [Table III(b)] which decrease to a degree upon reprocessing. To understand the phenomenon, the overall CLD for both of the TPVs has been measured before and after reprocessing. Further it has been found that there is a 0.8×10^{-5} mol/mL increase in CLD in case of SEV cured TPVs upon first reprocessing [shown in Figure 2(a)]. However, the change in CLD is marginal (approximately 0.10×10^{-5} mol/mL) for EV cured TPVs [shown in Figure 2(b)]. These are attributed to the post curing of the SEV cure TPVs by overshadowing the influence of degradation because of heat and mechanical shearing and thus, leading to a significant improvement in mechanical properties [Table III(a)] due to increase in elasticity of the elastomeric network after reprocessing. However, reprocessing causes a slight decrease in mechanical properties [Table III(b)] for EV cured TPVs which is due to the attainment of optimum cure level during initial dynamic vulcanization and further heat and mechanical treatments of the materials might cause an extent of degradation of the blend components.

Morphology Study

Scanning Electron Microscopy. To investigate the morphology developed during the TPV formation SEM study has been conducted with the cryogenically fractured and etched specimens and the images are given in Figure 3(a,b) for SEV cured TPVs and Figure 3(c,d) for EV cured TPVs. The mass fraction extraction during the solvent etching process from the respective TPVs was calculated by measuring the initial and final weight of the respective specimens (before and after etching) and it was found that the extracted mass fraction is approximately equivalent to the original mass fraction calculated in the respective TPVs. Moreover, the self supporting nature of the unextracted part after solvent etching indicates the formation of co-continuous morphology in the TPV systems.[27–29] Now, upon magnification of the initial images [Figure 3(a,c)] it was found that for Figure 3(b) there exists some elongated rubber particle which is absent in case of Figure 3(d). It is well-known that higher CLD is making the elastomeric phase more elastic in nature. Therefore, in case of EV cured TPV (SST 2) having higher elasticity of the elastomeric network [Figure 3(d)], the shearing action during mixing is not quite enough to achieve the critical stress[30] which would cause the cross-linked (predominantly mono-sulphide linkages of higher bond strength) elastomeric phase to break up and to attain the droplet-like morphology. In contrast, the SEV cured TPV (SST 1) also fails to achieve the critical stress, but the reduced elasticity of the cross-linked (di-sulphide and poly-sulphide linkages having lower bond strength) elastomeric network reduces the critical stress requirement and thus it ends-up with co-continuous morphology with elongated rubber particles [Figure 3(b)]. These morphological observations well agree (139% improvement in elongation at break for SST 1 compared to SST 2) with the mechanical property obtained for the TPVs (Table II).

Figure 4(a,b) demonstrates the SEM images of the SEV and EV cured TPVs after reprocessing. The cryogenically fractured and etched specimens have been subjected to the morphological

Table III. Mechanical Properties of TPVs After Reprocessing

Sample name	Tensile strength (MPa)	EB (%)	100% Modulus (MPa)	200% Modulus (MPa)	300% Modulus (MPa)	Hardness (shore A)
(a) SEV cured TPVs						
SST 1	4.9 (0.62)	672 (79.79)	0.9 (0.03)	1.4 (0.03)	2.0 (0.05)	52 (0.84)
SST 1R	6.3 (0.71)	666 (54.93)	1.1 (0.04)	1.6 (0.07)	2.3 (0.11)	53 (0.71)
(b) EV cured TPVs						
SST 2	4.8 (0.38)	533 (42.03)	1.1 (0.03)	1.7 (0.06)	2.6 (0.09)	55 (0.71)
SST 2R	4.4 (0.62)	510 (38.24)	1.0 (0.02)	1.5 (0.06)	2.1 (0.12)	55 (0.74)

Standard deviation values for five numbers of test specimens are given in parenthesis.
R, TPV after first reprocessing.

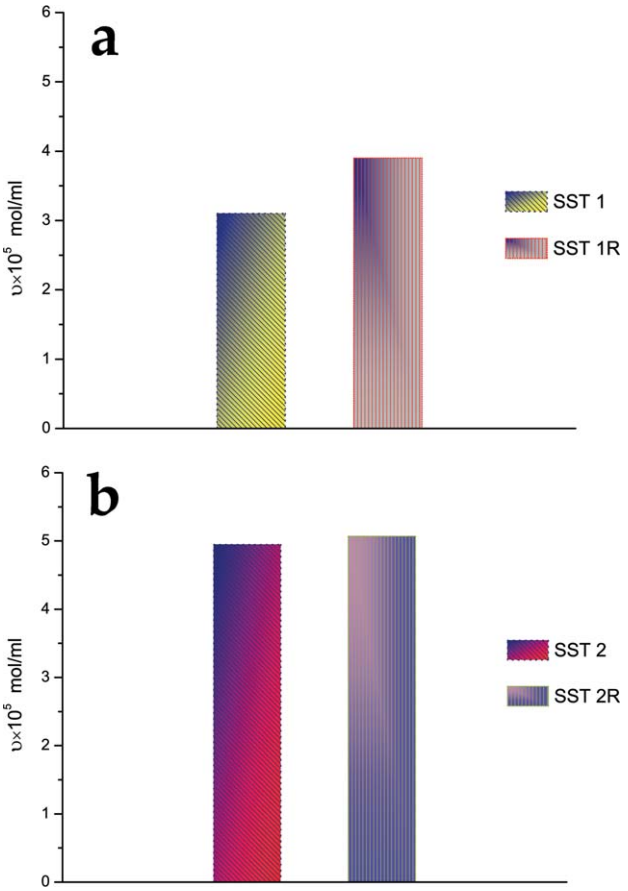

Figure 2. Overall Cross-link density for SEV cured TPV (a) before and after reprocessing and EV cured TPV (b) before and after reprocessing. [Color figure can be viewed in the online issue, which is available at wileyonlinelibrary.com.]

studies after proper drying. From the SEM image [Figure 4(a)] it is understood that reprocessing causes the formation of dispersed elastomeric particles along with the continuous rubber counterpart in case of SEV cured TPV (SST 1R). It is quite evident that the shear stress generated during the reprocessing is sufficient enough to break some of the elongated elastomer particles [Figure 3(b)] into small micro-domains and thus leading to the formation of droplet-like morphology along with co-continuous morphology. This may also be the reason for increase in mechanical property after first reprocessing for the SEV cured TPVs [Table III(a)]. On the contrary, reprocessing does not make any significant change in the EV cured TPVs [Figure 4(b)] and this is also the explanation for the unchanged mechanical property [Table III(b)] obtained for the EV cured TPVs upon reprocessing.

Atomic Force Microscopy. To confirm the morphology development during mixing, further investigation has been made with AFM for the sulfur cured TPV systems. Figure 5(a,b) represent the phase morphology of the SEV cured TPV (SST 1) and EV cured TPV (SST 2) systems, respectively. The light yellow regions in the phase and topography images represent cross-linked rubber particles, and the brown region represents the TPE phase. From the phase images it is clearly identified that both the phases are continuous leading to the formation of co-continuous morphology in both the TPV systems.

The morphological development for SEV and EV cured TPVs after reprocessing is depicted in Figure 6. The thin films were subjected to the morphological studies after proper cleaning and drying. Figure 6(a,b) represents the phase morphology of the SEV cured TPV (SST 1R) and EV cured TPV (SST 2R) systems, respectively after reprocessing. From the AFM phase image [Figure 6(a)] it is evident that reprocessing causes the formation of dispersed elastomeric particles along with the continuous rubber counterpart in case of SEV cured TPV (SST 1R). On the other hand, Figure 6(b) depicts no significant change in phase morphology for the EV cure TPVs upon reprocessing. All of these results are in well accordance with the SEM observations shown in Figure 4.

Melt Rheological Study

Complex shear modulus (G*) as a function of frequency and double strain amplitude at 120°C for TPVs are shown in the Figures. 7 and 8, respectively.[31,32] From the figures it can be clearly observed that with increasing frequency the complex shear modulus (G*) of the TPVs has increased (Figure 7). However, the increase is higher in case of TPV which is EV cross-linked (SST 2) compared to the SEV cured counterpart (SST 1). The frequency-dependence of the modulus is a result of chain and segment mobility in the material. At low frequencies, the polymer chains can follow the applied strain without delay and without loss of energy, because at the terminal zone[27,28] the enforced chain movements are equal to the applied frequency. With increasing frequencies of the applied strain, entanglements are no longer able to follow the applied strain and they act as temporary cross-links and thus the material shows elasticity. This region of a constant storage modulus is called the rubber plateau. Finally at the high frequency, the material has a high modulus, as a result of the rigidity of the polymer chains at these high frequencies. The molecules are not flexible enough to follow the applied strain.[33] Now, rubber vulcanizates always remain within this rubber plateau zone during the frequency scan and thus the G* value remains almost unchanged. On the other hand, the TPE (S-EB-S) present in the TPVs behaves accordingly as per the theory during the frequency scan, but the presence of cross-linked elastomeric phase makes the responses incongruous. Higher CLD in the elastomeric phase makes the TPVs more elastic in nature. Therefore, at high frequency the material becomes rigid and fails to follow the applied strain and thus depicts higher complex shear modulus (G*) value. From Figure 2 we have seen that the CLD is the highest for SST 2 followed by SST 1 and thus the TPVs are following the same trend during frequency sweep study. But, the same experiment with the reprocessed specimens reveals out some atypical observations. The complex shear modulus (G*) curve has become steeper [Figure 7(a)] and registered distinctively higher value for the SEV cured reprocessed (SST 1R) TPV compared to the initial TPV curve (SST 1). This is due to the increase in elasticity of the TPV network as is evident from Figure 2(a). On the other hand, EV cured reprocessed TPVs (SST 2R) have depicted marginal improvement [Figure 7(b)] in G* value due to

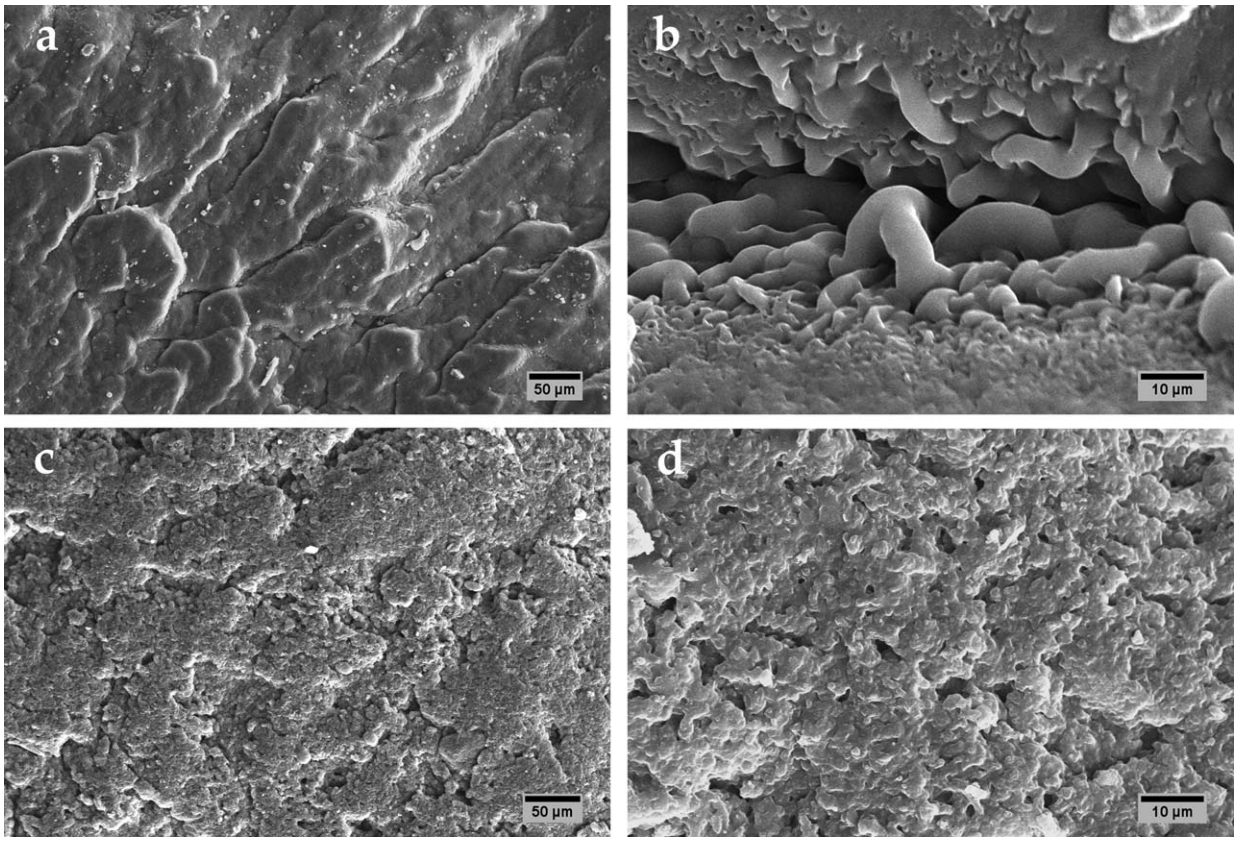

Figure 3. SEM photographs of sulfur cured S-EB-S and S-SBR TPVs after solvent etching: (a) and (b) SEV cured TPVs at 500× and 3000× magnifications & (c) and (d) EV cured TPVs at 500× and 3000× magnifications, respectively.

possessing comparable CLD values upon reprocessing [Figure 2(b)].

From the theory of strain-dependence of the Payne effect (Figure 9) it is well known that the main contributions to the complex shear modulus (G*) are the hydrodynamic effect, the polymer network, the filler–polymer and the filler–filler interaction. Since the subjected TPVs are devoid of filler particles, therefore the effect of polymer network during the strain sweep becomes more significant and the same has been shown for the respective TPVs, Figure 8. polymer network formation is a strain-independent contribution of the rubber network and it is the result of the proportionality of the shear modulus to νRT, where ν is the number of moles of elastically effective network chains per unit volume, as a result of vulcanization.[34] This effect can be called as Payne-like effect and from Figure 8 it can clearly seen that the complex shear modulus (G*) is increasing with the increase in ν value within the dynamic strain range. Here again, it is interesting to note that like frequency sweep the complex shear modulus (G*) at low strain level has increased [Figure 8(a)] for the reprocessed SEV cured TPV (SST 1R), where as it is marginally higher for SST 2R with their initial counterparts [Figure 8(b)]. The same argument of increase in cross-linking density is responsible for the observed phenomenon, but along with this the so called hydrodynamic effect appears to be operative. As mentioned earlier, the TPVs under consideration are unfilled ones, but the morphological observations (SEM and AFM) reveal the formation of partially droplet type morphology in case of SEV cured TPVs upon reprocessing [Figures. 4(a) and 6(a)]. These spherical rubber particles are acting as reinforcing fillers to the thermoplastic matrix and partially assisting in the increase in complex shear modulus (G*) for SST 1R. The same effect is absent in case of EV cured TPVs due to the formation of co-continuous type morphology [Figures. 4(b) and 6(b)] upon reprocessing.

For the typical pseudo-plastic materials the complex shear viscosity (η^*) decreases as a function of frequency. From Figure 10 it is evident that with the increase in crosslink-density there is an increase in complex viscosity (η^*) and followed by a gradual decrease in η^* with the increasing frequency indicating typical pseudo-plastic behavior. Here also, like frequency and strain sweep the complex viscosity (η^*) at low frequency has increased [Figure 10(a)] for the reprocessed SEV cured TPV (SST 1R), where as it is almost unchanged [Figure 10(b)] for SST 2R with their initial counterparts. Thus, the results again confirm that reprocessing causes a significant increase in cross-linking density for the SEV cured (SST 1) TPVs which eventually ends up with higher initial viscosity for the reprocessed TPVs (SST 1R) systems.

Dynamic Mechanical Analysis

All of the results obtained from morphological observations by SEM and AFM, cross-linking density study, physico-mechanical

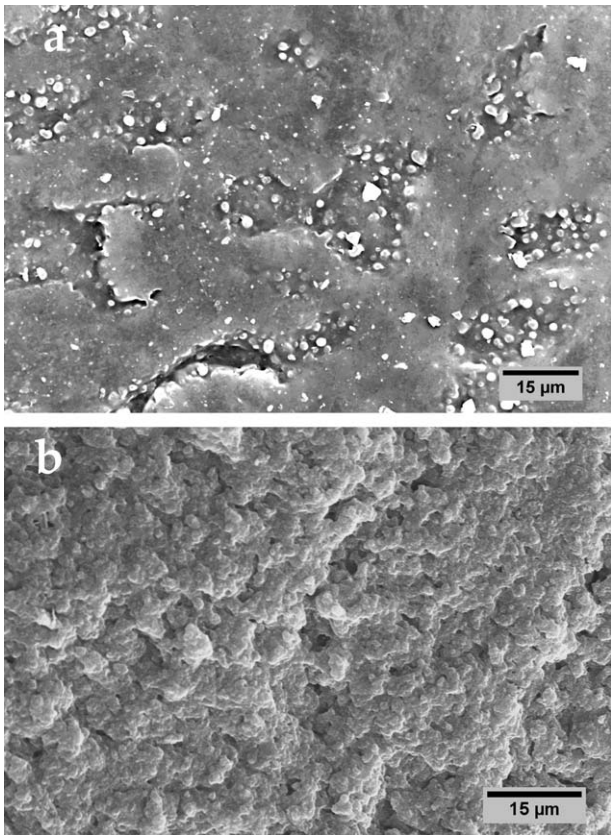

Figure 4. SEM images of sulfur cured S-EB-S and S-SBR TPVs after solvent etching: (a) SEV cured TPVs and (b) EV cured TPVs, respectively after reprocessing.

property, and melt rheology study suggest that reprocessing causes a definite increase in cross-linking density as well as elasticity and thereby leads to the significant improvement in final properties in case of SEV cured TPVs. Similar effect has been established through dynamic mechanical analysis like melt rheology study. In melt rheology, the matrix phase got melted and then it was easier to follow the effect of morphology change by monitoring the complex shear modulus (G*). But, dynamic mechanical analysis conducted at 25°C failed to nullify the effect of matrix phase contribution entirely while collecting the dynamic responses provided by the cross-linked elastomeric phases of different morphology and it is well evident from the temperature sweep study (Figure 11) that the storage modulus (E′) values (Table IV) obtained for the TPVs under investigation (at 25°C) are very much comparable to the virgin S-SBR vulcanizate and S-EB-S used as the initial raw materials for TPV preparation. Thus, there is always an interference produced by the matrix phase and it leads to a weak dynamic response produced by the cross-linked elastomeric phase. However, it is still substantial to interpret the microstructural effects on the respective TPVs from the viscoelastic studies describe below.

Creep Study. Literature shows that nothing has been reported so far on creep behavior of S-SBR/S-EB-S TPV systems. Thus, there is wide scope of research opportunity in this field in order to explore the effect of microstructure change on the creep behavior of TPV. In addition, creep study is very much essential from its fundamental point of view while application in automobile ancillaries is taken under consideration. Polymers being viscoelastic materials show "creep" behavior when subjected to a constant stress. The stress–strain curves are modeled by Kelvin and Voigt as[25]

$$J(t)=J_0+\sum_{i=1}^{n} J_i\left[1-e^{-t/\tau_i}\right], \quad (5)$$

where $J(t)$ and J_0 are the creep compliance after time t and instantaneous creep compliance, and J_i and τ_i are the constants characteristic of the system. The strain–time plot for the TPVs is given in Figure 12 which shows good coherence with the characteristic strain–time plot for viscoelastic materials. The plots are in accordance with the various stages of creep viz., primary creep due to relatively high strain rate and the secondary creep with steady state attainment. However, the tertiary creep leading to yielding is absent for all of the samples. Figure 12

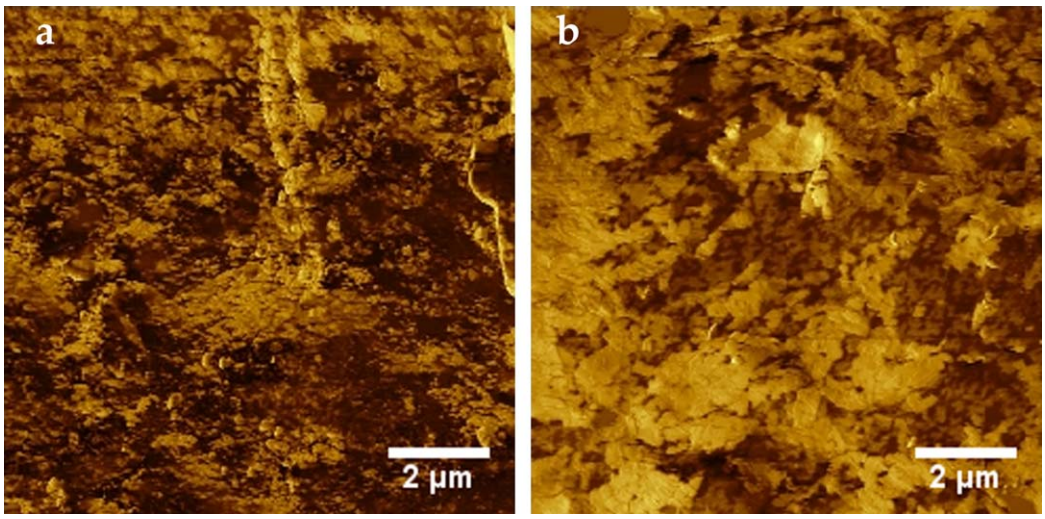

Figure 5. AFM phase images (a) and (b) of SEV cured TPV and EV cured TPV respectively [scan area 10 × 10 μm^2]. [Color figure can be viewed in the online issue, which is available at wileyonlinelibrary.com.]

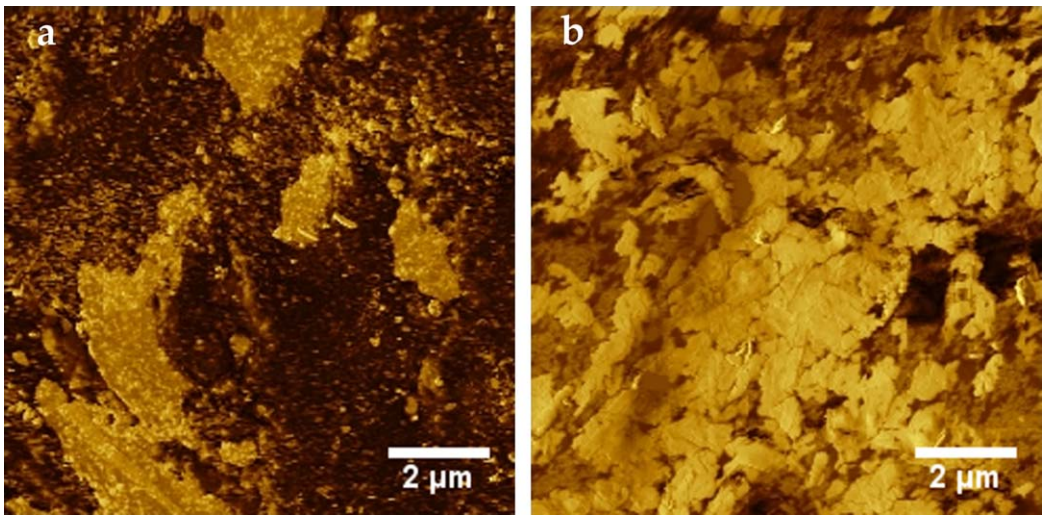

Figure 6. AFM phase images (a) and (b) of SEV cured TPV and EV cured TPV, respectively after reprocessing [scan area 10 × 10 μm^2]. [Color figure can be viewed in the online issue, which is available at wileyonlinelibrary.com.]

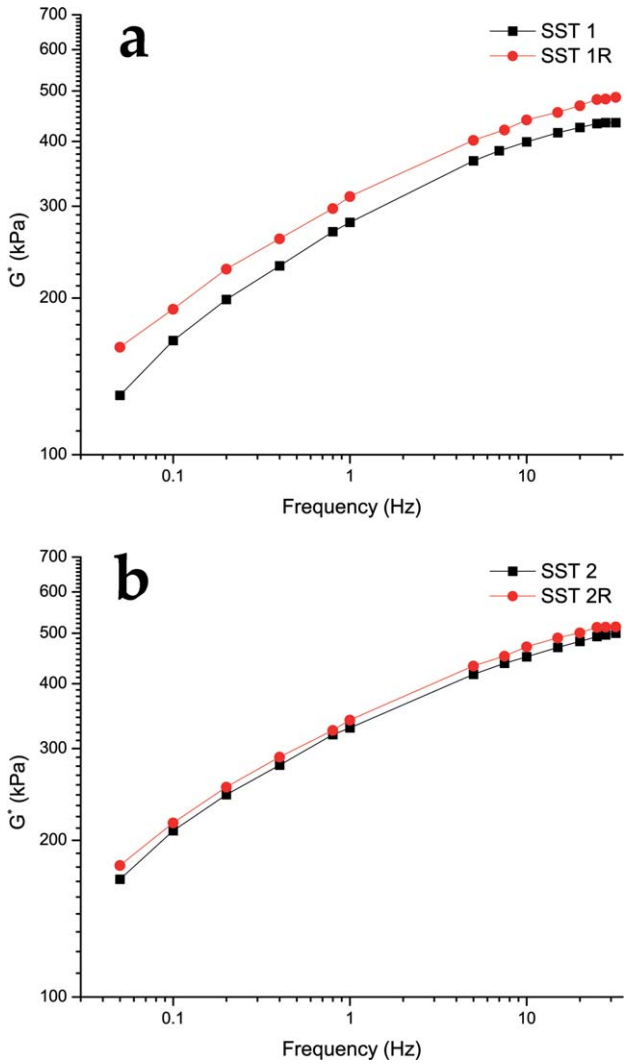

Figure 7. Variation of complex modulus (G*) as a function of frequency of (a) SEV cured TPVs and (b) EV cured TPVs before and after reprocessing. [Color figure can be viewed in the online issue, which is available at wileyonlinelibrary.com.]

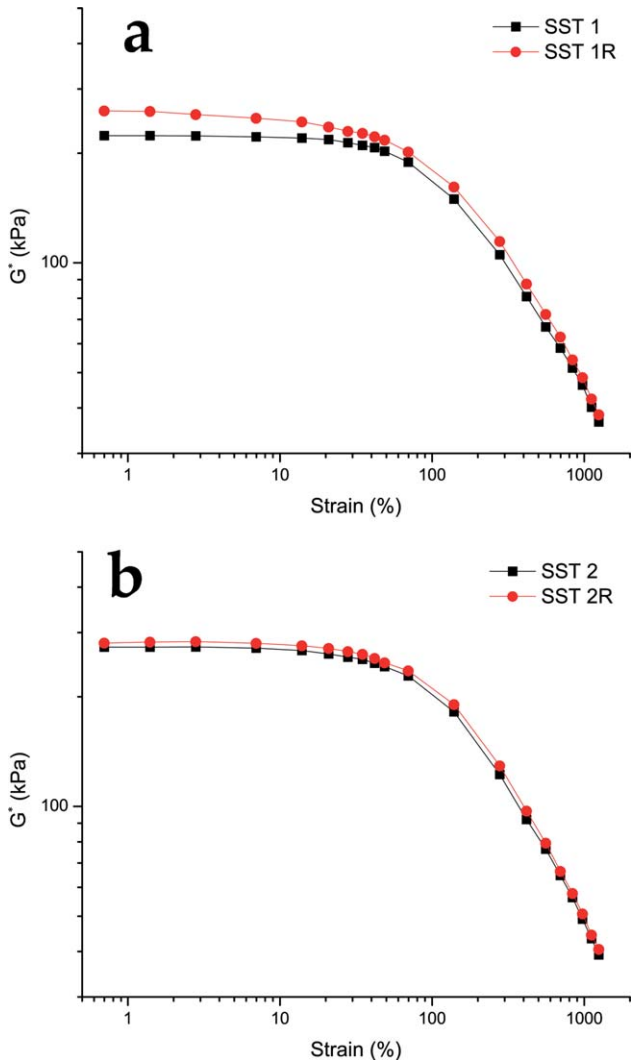

Figure 8. Variation of complex modulus (G*) as a function of strain amplitude of (a) SEV cured TPVs and (b) EV cured TPVs before and after reprocessing. [Color figure can be viewed in the online issue, which is available at wileyonlinelibrary.com.]

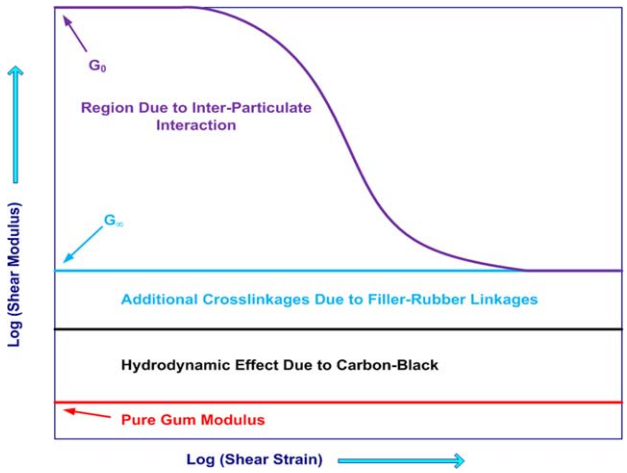

Figure 9. The G*-modulus as a function of strain for a reinforced rubber vulcanizate. [Color figure can be viewed in the online issue, which is available at wileyonlinelibrary.com.]

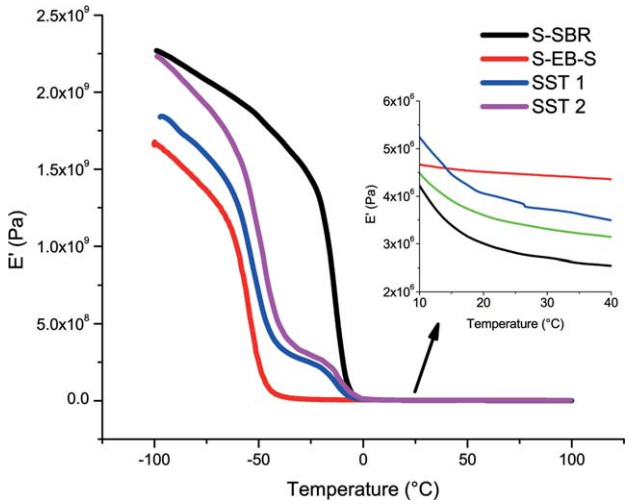

Figure 11. Temperature dependence of storage modulus (E′) of dynamically vulcanized blends, rubber vulcanizate and pristine TPE. [Color figure can be viewed in the online issue, which is available at wileyonlinelibrary.com.]

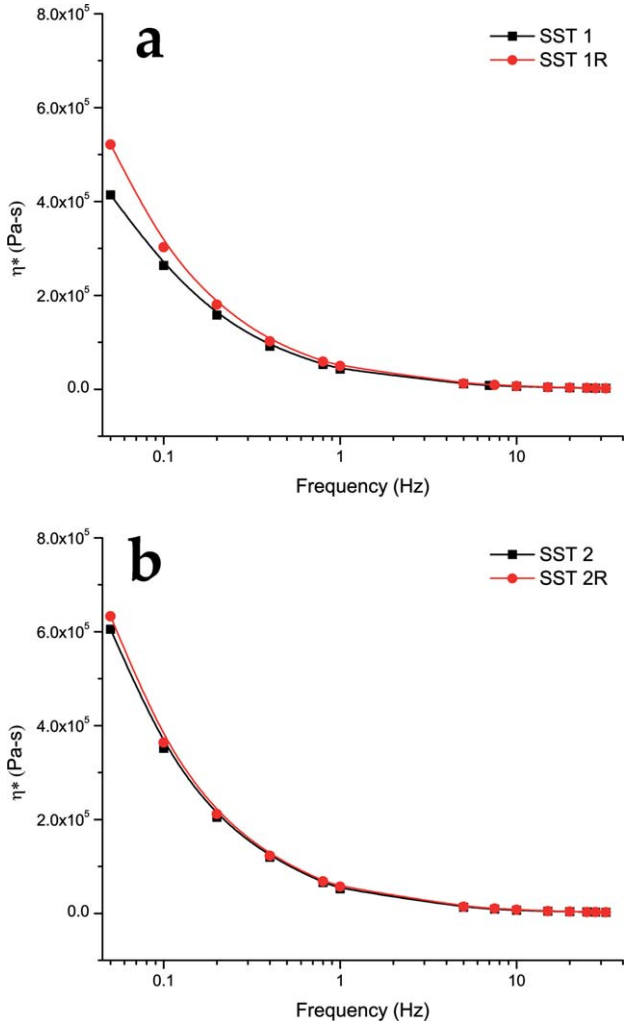

Figure 10. Variation of complex shear viscosity (η^*) as a function of frequency of (a) SEV cured TPVs and (b) EV cured TPVs before and after reprocessing. [Color figure can be viewed in the online issue, which is available at wileyonlinelibrary.com.]

depicts the representative strain response to creep and recovery for the TPVs. Application of constant stress leads to an instantaneous deformation which is followed by a continuous and steady increase in strain as a function of time with a subsequent attainment of steady-state creep. On withdrawal of the stress, there is a sudden fall in strain which is followed by a smooth decrease due to elastic recovery of the polymeric material. In creep experiment the strain recovery is mostly below 100% because of the viscous nature of the material. For the SEV cured TPVs [Figure 12(a)], it is very much well understood that there is a significant change in strain response for the TPVs before and after reprocessing (SST 1 and SST 1R), while the change is marginal [Figure 12(b)] for EV cured TPVs (SST 2 and SST 2R). Similar explanation of CLD variation and microstructural changes are valid as described in melt rheology study. In addition, a comparative analysis of creep compliance for the all TPVs before and after reprocessing is given in Figure 13. It is quite vivid that the increase in CLD and the formation of partially droplet type morphology actually causes an increase in elasticity of the polymeric networks for SEV cured TPVs, which is followed by a drastic fall in the magnitude of creep compliance. This effect is not prominent for EV cured TPVs having unaltered CLD and morphology before and after reprocessing. For instance, for the SEV cured and EV cured TPVs, there is 20 and 3% decrease in this parameter. This indicates improved creep resistance for the SEV cured TPVs after reprocessing which is almost constant for the EV cured ones. The recovery compliance also follows the same trend as that of creep compliance.

Stress Relaxation Study. Like creep study, similar kind of behavior was observed during stress relaxation study for the S-SBR/S-SE-S TPV systems. The stress–strain curves are modeled by Maxwell as[25]

$$E(t) = \sum_{i=1}^{n} E_i e^{-t/\tau_i}, \quad (6)$$

where E(t) is the relaxation modulus after time t and E_i and τ_i are the constants characteristic of the system. The stress–time plot for

Table IV. Dynamic Storage Modulus Obtained from Temperature Sweep Study in DMA: Analysis of TPVs, S-SBR Vulcanizate, and S-EB-S

	Storage modulus (E′) (MPa)
Sample name	25°C
S-SBR	2.79
S-EB-S	4.50
SST 1	3.41
SST 2	3.90

the TPVs is given in Figure 14 which shows good coherence with the characteristic stress–time plot for viscoelastic materials. Similar to the creep experiment, there is a prominent change in stress response [Figure 14(a)] for the SEV cured TPVs before and after reprocessing (SST 1 and SST 1R), while the change is marginal [Figure 14(b)] for EV cured TPVs (SST 2 and SST 2R). The recovery curves also follow the same trend as that of relaxation

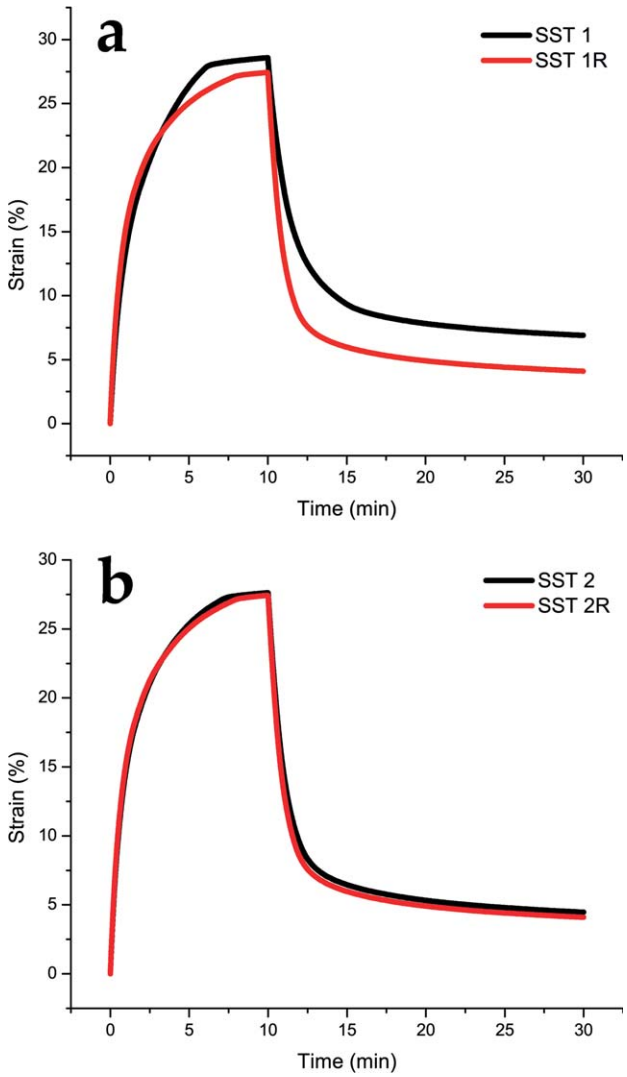

Figure 12. Comparison of strain versus time curves for (a) SEV and (b) EV cured TPVs before and after reprocessing (under a constant stress of 0.3 MPa and at 25°C temperature). [Color figure can be viewed in the online issue, which is available at wileyonlinelibrary.com.]

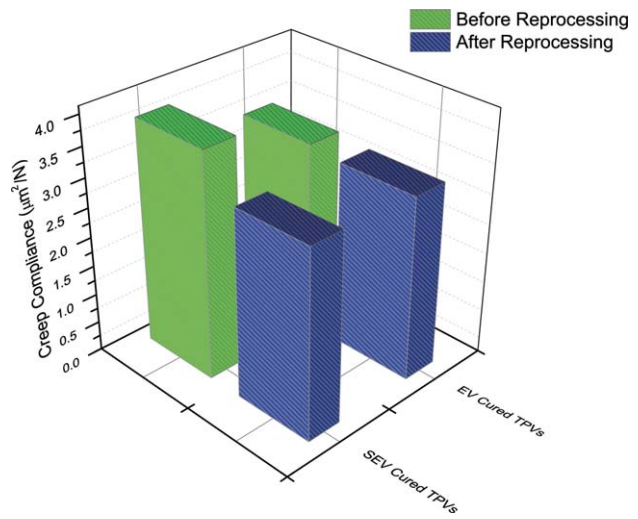

Figure 13. Comparison of the creep compliance of SEV and EV cured TPVs before and after reprocessing (constant stress of 0.3 MPa and a temperature of 25°C were imposed). [Color figure can be viewed in the online issue, which is available at wileyonlinelibrary.com.]

curves. These results once again revalidate the effect of CLD and morphology reorientation on the viscoelastic properties of TPVs based on S-SBR and S-EB-S systems as evident from the microscopic observations by SEM and AFM.

CONCLUSIONS

TPVs based on S-EB-S and S-SBR blends have been prepared by selective curing of S-SBR phase and by adopting semi-efficient (SEV) and efficient (EV) vulcanization systems. SEV cured TPVs showed better physico-mechanical property and it has been explained through morphological study by SEM. Both of the TPVs initially formed co-continuous morphology, but reprocessing causes the formation of partially droplet morphology in case of SEV cured TPVs by reducing the critical shear stress while mixing due to the formation of di-sulphide and poly-sulphide linkages. The droplet morphology formation is also responsible for an improvement in physico-mechanical properties for the SEV cured TPVs upon reprocessing. Moreover, a detailed analysis has been conducted to investigate the effect of microstructure changes on the melt rheology and dynamic viscoelastic properties of the TPVs of interest. Melt rheology study concludes a definite increase in complex shear modulus (G^*) and shear viscosity (η^*) while performing frequency sweep and strain sweep for the SEV cured TPV system upon reprocessing. In contrast, the effect is less significant in case of EV cured TPVs. Similarly, a prominent change in creep compliance and relaxation modulus has been observed for the SEV cured system unlike EV cured ones due to the increase in CLD and the change in morphology. This investigation leads to a new avenue into morphology-mechanical-rheological-viscoelastic property correlation in TPVs systems.

ACKNOWLEDGMENTS

We thank CEAT Limited for the financial support in this project. Thanks to Dr, H. de Groot (Kraton Polymer Research, Belgium) for supplying us free sample of S-EB-S. We are thanking Central

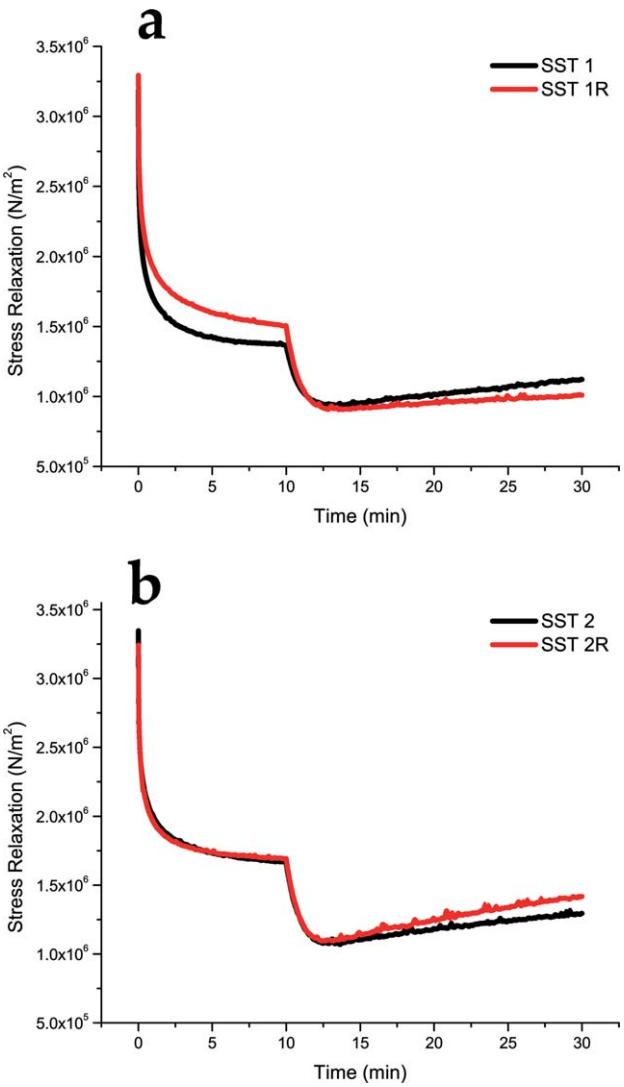

Figure 14. Comparison of stress versus time curves for (a) SEV and (b) EV cured TPVs before and after reprocessing (under a constant strain of 0.05% and at 25°C temperature). [Color figure can be viewed in the online issue, which is available at wileyonlinelibrary.com.]

Research Facility (IIT Kharagpur, India) for providing the morphology characterization facility by means of SEM and AFM. Last but not the least; we thank Dr S. Chattopadhyay (Rubber Technology Centre, IIT Kharagpur, India) and Dr R. Mukherjee (Chemical Engineering Deparment, IIT Kharagpur, India) for their valuable discussion and support.

REFERENCES

1. Karger-Kocsis, J. In Polymer Blends and Alloys; Shonaike, G. O.; Simon, G. P., Eds.; Marcel Dekker AG: New York, **1999**; Chapter *5*, p 125.
2. van Duin, M. *Macromol. Symp.* **2006**, *233*, 11.
3. Bousmina, M.; Muller, R. *Rheol. Acta* **1996**, *35*, 369.
4. Abdou-Sabet, S.; Puydak, R. C.; Rader, C. P. *Rubber Chem. Technol.* **1996**, *69*, 476.
5. Antunes, C. F.; Machado, A. V.; van Duin, M. *Eur. Polym. J.* **2011**, *47*, 1447.
6. Brostow, W.; Grguric, T. H.; Olea-Mejia, O.; Rek, V.; Unni, J. *e-Polymer* **2008**, *8*, 355.
7. Grein, C.; Gahleitner, M.; Bernreitner, K. *eXPRESS Polym. Lett.* **2012**, *6*, 688.
8. Deniz, V.; Karakaya, N.; Ersoy, O. G. *Soc. Plast. Eng.* **2009**, *1*.
9. Sengupta, P.; Noordermeer, J. W. M. *Polymer* **2005**, *46*, 12298.
10. Sengupta, P.; Noordermeer, J. W. M. *Macromol. Rapid Commun.* **2005**, *26*, 542.
11. Sengers, W. G. F.; Sengupta, P.; Noordermeer, J. W. M.; Picken, S. J.; Gotsis, A. D. *Polymer* **2004**, *45*, 8881.
12. Sengers, W. G. F.; Wübbenhorst, M.; Picken, S. J.; Gotsis, A. D. *Polymer* **2005**, *46*, 6391.
13. Ahmad, Z.; Kumar, K. D.; Saroop, M.; Preschilla, N.; Biswas, A.; Bellare, J. R.; Bhowmick, A. K. *Polym. Eng. Sci.* **2010**, *50*, 331.
14. Picchioni, F.; Aglietto, M.; Passaglia, E.; Ciardelli, F. *Polymer* **2002**, *43*, 3323.
15. Soares, B. G.; Santos, D. M.; Sirqueira, A. S. *eXPRESS Polym. Lett.* **2008**, *2*, 602.
16. Nakason, C.; Worlee, A.; Salaeh, S. *Polym. Test.* **2008**, *27*, 858.
17. Zhang, X.; Huang, H.; Zhang, Y. *J. Appl. Polym. Sci.* **2002**, *85*, 2862.
18. Flory, P. J.; Rehner, J. *J. Chem. Phys.* **1943**, *11*, 512.
19. Mullins, L.; Tobin, N. R. *J. Appl. Polym. Sci.* **1965**, *9*, 2993.
20. Chatterjee, T.; Wiessner, S.; Naskar, K.; Heinrich, G. *eXPRESS Polym. Lett.* **2013**, *8*, 220.
21. Babu, R. R.; Singha, N. K.; Naskar, K. *J. Polym. Res.* **2010**, *18*, 31.
22. Babu, R. R.; Naskar, K. *Adv. Polym. Sci.* **2011**, *239*, 219.
23. Barlkanl, M.; Hepburn, C. *Iranian J. Polym. Sci. Technol.* **1992**, *1*, 1.
24. Dikland, H. Novel Co-Agents for Improved Properties in Peroxide Cure of Saturated Elastomers. Ph.D. Thesis, University of Twente, The Netherlands, **1992**.
25. Shaw, M. T.; MacKnight, W. J. Introduction to Polymer Viscoelasticity, 3rd ed.; John Wiley & Sons, Inc., Hoboken, New Jersey **2005**; Chapter 2, p 51.
26. Li, Y.; Oono, Y.; Kadowaki, Y.; Inoue, T.; Nakayama, K.; Shimizu, H. *Macromolecules* **2006**, *39*, 4195.
27. Gubbels, F.; Blacher, S.; Vanlathem, E.; Jerome, R.; Deltour, R.; Brouers, F.; Teyssie, P. *Macromolecules* **1995**, *28*, 1559.
28. Pötschke, P.; Paul, D. R. *J. Macromol. Sci., Part C* **2003**, *43*, 87.
29. Lagrève, C.; Feller, J. F.; Linossier, I.; Levesque, G. *Polym. Engi. Sci.*, **2001**, *41*, 1124.
30. l'Abee, R. M. A.; van Duin, M.; Spoelstra, A. B.; Goossens, J. G. P. *Soft. Matter.* **2010**, *6*, 1758.
31. Shibulal, G. S.; Naskar, K. *J. Appl. Polym. Sci.* **2013**, *128*, 4151.
32. Babu, R. R.; Singha, N. K.; Naskar, K. *J. Appl. Polym. Sci.* **2010**, *117*, 1578.
33. Menard, K. P. Dynamic Mechanical Analysis: A Practical Introduction, 1st ed.; CRC Press LLC, Boca Raton, Florida, **1999**; Chapter 4, p 61.
34. Hui, S.; Chaki, T. K.; Chattopadhyay, S. *Polym. Comp.* **2010**, *31*, 377.